A Hybrid Source for Deterministic Generation of Atom-Photon Entangled States

Priyanshu Tiwari,[1,2,3,*] Aleksa Krstić,[3] Frank Setzpfandt,[3,4] Robert Löw,[5] and Sina Saravi[1,2,6,3]

[1] *Heinz Nixdorf Institute, Paderborn University, Fürstenallee 11, 33102 Paderborn, Germany*
[2] *Department of Electrical Engineering and Information Technology, Paderborn University, Warburger Straße 100, 33098 Paderborn, Germany*
[3] *Institute of Applied Physics, Abbe Center of Photonics, Friedrich Schiller University Jena, Albert-Einstein-Straße 15, 07745 Jena, Germany*
[4] *Fraunhofer Institute for Applied Optics and Precision Engineering, Albert-Einstein-Straße 7, 07745 Jena, Germany*
[5] *Physikalisches Institut, Universität Stuttgart, Pfaffenwaldring 57, 70569 Stuttgart, Germany*
[6] *Institute for Photonic Quantum Systems (PhoQS), Paderborn University, Warburger Str. 100, 33098 Paderborn, Germany*

CONTENTS

S1. TIME-DEPENDENT PERTURBATION THEORY FOR $|\phi_1\rangle$

In this section, we analyze off-resonant parametric down-conversion(PDC) processes using time-dependent perturbation theory. For the PDC process in the regime $\Delta_1 \gg A_p$, higher-order cavity states are negligibly occupied, and only the state $|\phi_1\rangle$ is weakly populated. Therefore, the probability amplitude for $|\phi_1\rangle$ can be obtained using first-order time-dependent perturbation theory:

$$\begin{aligned} C^{(1)}_{\phi_1}(t) &= -\frac{i}{\hbar}\int_0^t \langle\phi_1|\,\hat{H}_{\mathrm{NL}}(t_1)\,|0\rangle\, dt_1 \\ &= -iA_p\sqrt{2}\int_0^t e^{-i\Delta_1 t_1}\, dt_1 \\ &= -i\frac{A_p}{\Delta_1}2\sqrt{2}e^{-i\frac{\Delta_1 t}{2}}\sin\frac{\Delta_1 t}{2} \end{aligned} \tag{S1}$$

The term $\langle\phi_1|\,\hat{H}_{\mathrm{NL}}(t_1)\,|0\rangle$ represents the transition amplitude per unit time at time t_1 for the cavity to be in the state $|\phi_1\rangle$. The total transition amplitude for the cavity state to evolve from $|0\rangle$ to $|\phi_1\rangle$ within time t is given by $C_{\phi_1}(t)$,

* priyanshu.tiwari@uni-paderborn.de

which is obtained as an integral over the $\langle\phi_1|\,\hat{H}_{\rm NL}(t_1)\,|0\rangle$. The absolute square gives the total transition probability for the cavity state to go from $|0\rangle$ to $|\phi_1\rangle$ within time t.

$$|C^{(1)}_{\phi_1}(t)|^2 = 8\frac{A_p^2}{\Delta_1^2}\sin^2\frac{\Delta_1 t}{2} \tag{S2}$$

The transition amplitude per unit time acquires a time-dependent phase due to the presence of detuning Δ_1. These phases vary on a time scale $\frac{1}{\Delta_1}$. Since A_p sets the characteristic time scale for the generation of the cavity states $|\phi_n\rangle$, in the regime $\Delta_1 \gg A_p$, the phases vary rapidly over this time scale. As a result, the rapidly varying phases cause the time-dependent probability amplitude contributions to the total transition amplitude arising from different times to become out of phase resulting in partial constructive and destructive interference over the integration interval, thereby preventing their coherent accumulation and leading to a very small net amplitude for the transition of the cavity state from vacuum $|0\rangle$ to $|\phi_1\rangle$.

S2. COUPLED DIFFERENTIAL EQUATION B/W VACUUM STATE $|0\rangle$ AND THE STATE $|\psi_{e_1,e_2}\rangle$ OBTAINED AFTER ADIABATIC ELIMINATION

In this section, we will derive the coupled differential Eq. (1) in the manuscript. The Hamiltonian of the system in the interaction picture is:

$$\begin{aligned}\hat{H}(t) &= \hat{H}_{NL}(t) + \hat{H}_{e\leftrightarrow g}(t)\\ \hat{H}(t) &= \hbar A_p\left[\hat{a}_L^\dagger\hat{b}_R^\dagger + \hat{a}_R^\dagger\hat{b}_L^\dagger\right]e^{-i\Delta_1 t} + \hbar\Omega\left[\hat{a}_L\,|e_1\rangle\langle g| - \hat{a}_R\,|e_2\rangle\langle g|\right]e^{i\Delta_2 t} + \text{H.c}\end{aligned} \tag{S3}$$

The initial state of the system is $|0,0,0,0,g\rangle \equiv |0;g\rangle$, where the cavity modes are in the vacuum state, and the atom is in the ground state. The Schrödinger equation describing the temporal dynamics of the system is:

$$i\hbar\frac{\partial\,|\psi(t)\rangle}{\partial t} = \hat{H}(t)\,|\psi(t)\rangle\,. \tag{S4}$$

We adopt the following ansatz for the system state $|\psi(t)\rangle$ at an arbitrary time t:

$$|\psi(t)\rangle = C_{0,g}(t)\,|0;g\rangle + C_1(t)\,|\phi_1;g\rangle + C_2(t)\,|\phi_2;g\rangle + C_{e_1,e_2}(t)\,|\psi_{e_1,e_2}\rangle + C_3(t)\,|\psi_1\rangle \tag{S5}$$

where $|0;g\rangle$, $|\phi_1;g\rangle$, $|\phi_2;g\rangle$, and $|\psi_{e_1,e_2}\rangle$ are the same as defined in the manuscript, and $|\psi_1\rangle = \sqrt{\frac{1}{3}}\big(\,|1,0,0,2,e_1\rangle - |0,1,2,0,e_2\rangle\,\big) + \frac{1}{\sqrt{6}}\big(\,|0,1,1,1,e_1\rangle - |1,0,1,1,e_2\rangle\,\big)$.
The above ansatz is motivated by our numerical simulations, which show that the maximum probability of generating the target state $|\psi_{e_1,e_2}\rangle$ is achieved in the regime $A_p \ll \Delta_1$ (see Fig 4(b) and 4 (c) of the manuscript). In this large-detuning regime, the nonlinear coupling strength is much weaker than the detuning, strongly suppressing the population of higher-order excited states. As a result, the system dynamics are well described by the truncated basis above, allowing us to derive an effective description of the temporal evolution of the atom-photon entangled state $|\psi_{e_1,e_2}\rangle$. The differential equations governing the dynamics of these states are:

$$\begin{aligned}i\frac{\partial C_{0,g}}{\partial t} &= \sqrt{2}A_p e^{i\Delta_1 t}C_1(t)\\ i\frac{\partial C_1}{\partial t} &= \sqrt{2}A_p e^{-i\Delta_1 t}C_{0,g}(t) + \sqrt{6}A_p e^{i\Delta_1 t}C_2(t) + \Omega C_{e_1,e_2}(t)e^{-i\Delta_2 t}\\ i\frac{\partial C_2}{\partial t} &= \sqrt{6}A_p e^{-i\Delta_1 t}C_1(t) + \sqrt{2}\Omega C_3(t)e^{-i\Delta_2 t}\\ i\frac{\partial C_{e_1,e_2}}{\partial t} &= \Omega e^{i\Delta_2 t}C_1(t) + A_p\sqrt{3}C_3(t)e^{i\Delta_1 t}\\ i\frac{\partial C_3}{\partial t} &= \sqrt{2}\Omega C_2(t)e^{i\Delta_2 t} + A_p\sqrt{3}C_{e_1,e_2}(t)e^{-i\Delta_1 t}\end{aligned} \tag{S6}$$

Next, we transform to a rotating frame by redefining the probability amplitudes so as to remove the rapidly oscillating phase factors from the coupled differential equations. The transformed amplitudes are given by

$$C_1'(t) = C_1(t)e^{i\Delta_1 t}, \qquad C_2'(t) = C_2(t)e^{i2\Delta_1 t},$$

$$C'_{e_1,e_2}(t) = C_{e_1,e_2}(t)e^{i(\Delta_1-\Delta_2)t}, \qquad C'_3(t) = C_3(t)e^{i(2\Delta_1-\Delta_2)t}.$$

After substituting these transformed probability amplitudes into the above set of differential equations, we obtain:

$$\begin{aligned}
i\frac{\partial C_{0,g}}{\partial t} &= \sqrt{2}A_pC'_1(t) \\
i\frac{\partial C'_1}{\partial t} &= -\Delta_1C'_1(t) + \sqrt{2}A_pC_{0,g}(t) + \sqrt{6}A_pC'_2(t) + \Omega C'_{e_1,e_2}(t) \\
i\frac{\partial C'_2}{\partial t} &= -2\Delta_1C'_2(t) + \sqrt{6}A_pC'_1(t) + \sqrt{2}\Omega C'_3(t) \\
i\frac{\partial C'_{e_1,e_2}}{\partial t} &= -(\Delta_1-\Delta_2)C'_{e_1,e_2} + \Omega C'_1(t) + A_p\sqrt{3}C'_3(t) \\
i\frac{\partial C'_3}{\partial t} &= -(2\Delta_1-\Delta_2)C'_3(t) + \sqrt{2}\Omega C'_2(t) + A_p\sqrt{3}C'_{e_1,e_2}(t)
\end{aligned} \tag{S7}$$

We now impose the condition $\Delta_1 = \Delta_2$ and assume $\Delta_1 \gg \Omega$, while maintaining the condition $\Delta_1 \gg A_p$.
Under these conditions, the intermediate states $|\phi_1\rangle$, $|\phi_2\rangle$, and $|\psi_1\rangle$ evolve on a fast timescale set by $1/\Delta_1$, whereas the amplitudes of the slow states $|0;g\rangle$ and $|\psi_{e_1,e_2}\rangle$ vary on much longer timescales set by $1/A_p$ and $1/\Omega$. As a result, the intermediate states can be treated as fast variables and adiabatically eliminated, since they rapidly reach their quasi-steady-state values and become functions of the slow variables [S1].
Note: after imposing the condition $\Delta_1 = \Delta_2$, we get $C'_{e_1,e_2}(t) = C_{e_1,e_2}(t)$.
The first step in adiabatically eliminating these intermediate states is to set the time derivatives of C'_1, C'_2 and C'_3 to zero and obtain their quasi-steady-state expressions.

$$\begin{aligned}
i\frac{\partial C_{0,g}}{\partial t} &= \sqrt{2}A_pC'_1(t) \\
0 &= -\Delta_1C'_1(t) + \sqrt{2}A_pC_{0,g}(t) + \sqrt{6}A_pC'_2(t) + \Omega C'_{e_1,e_2}(t) \\
0 &= -2\Delta_1C'_2(t) + \sqrt{6}A_pC'_1(t) + \sqrt{2}\Omega C'_3(t) \\
i\frac{\partial C_{e_1,e_2}}{\partial t} &= \Omega C'_1(t) + A_p\sqrt{3}C'_3(t) \\
0 &= -\Delta_1C'_3(t) + \sqrt{2}\Omega C'_2(t) + A_p\sqrt{3}C_{e_1,e_2}(t)
\end{aligned} \tag{S8}$$

The quasi-steady state expression for $C'_1(t)$ is:

$$C'_1(t) = \frac{\sqrt{2}A_p}{\Delta_1}C_{0,g}(t) + \frac{\sqrt{6}A_p}{\Delta_1}C'_2(t) + \frac{\Omega}{\Delta_1}C'_{e_1,e_2}(t). \tag{S9}$$

Since the slowly varying amplitude $C_{0,g}(t)$ is of order unity, i.e., $C_{0,g}(t) = \mathcal{O}(1)$ because in the limit $A_p/\Delta_1 \to 0$ the minimum value of $C_{0,g}$ takes a finite value, it follows that $C'_1(t) = \mathcal{O}\left(\frac{A_p}{\Delta_1}\right)$. Under the adiabatic approximation, we neglect all terms of third and higher order in the parameters A_p/Δ and Ω/Δ.
The quasi-steady state expression for $C'_2(t)$ and $C'_3(t)$ is:

$$\begin{aligned}
C'_2(t) &= \frac{\sqrt{6}A_p}{2\Delta_1}C'_1(t) + \frac{\sqrt{2}\Omega}{2\Delta_1}C'_3(t) \\
C'_3(t) &= \sqrt{2}\frac{\Omega}{\Delta_1}C'_2(t) + \frac{A_p\sqrt{3}}{\Delta_1}C_{e_1,e_2}(t)
\end{aligned} \tag{S10}$$

Substitute the equation of $C'_3(t)$ into the equation for $C'_2(t)$,

$$\begin{aligned}
C'_2(t) &= \frac{\sqrt{6}A_p}{2\Delta_1}C'_1(t) + \frac{\sqrt{2}\Omega}{2\Delta_1}\left(\sqrt{2}\frac{\Omega}{\Delta_1}C'_2(t) + \frac{\sqrt{3}A_p}{\Delta_1}C_{e_1,e_2}(t)\right) \\
&= \frac{\sqrt{6}A_p}{2\Delta_1}C'_1(t) + \frac{\Omega^2}{\Delta_1^2}C'_2(t) + \frac{\sqrt{6}A_p\Omega}{2\Delta_1^2}C_{e_1,e_2}(t) \\
\left(1-\frac{\Omega^2}{\Delta_1^2}\right)C'_2(t) &= \frac{\sqrt{6}A_p}{2\Delta_1}C'_1(t) + \frac{\sqrt{6}A_p\Omega}{2\Delta_1^2}C_{e_1,e_2}(t).
\end{aligned} \tag{S11}$$

Rearranging the above equation gives

$$C_2'(t) = \frac{1}{1-\frac{\Omega^2}{\Delta_1^2}}\left[\frac{\sqrt{6}A_p}{2\Delta_1}C_1'(t) + \frac{\sqrt{6}A_p\Omega}{2\Delta_1^2}C_{e_1,e_2}(t)\right]. \tag{S12}$$

Since $\Omega/\Delta_1 \ll 1$, we expand the prefactor using the binomial expansion,

$$\frac{1}{1-\frac{\Omega^2}{\Delta_1^2}} = 1 + \frac{\Omega^2}{\Delta_1^2} + \mathcal{O}\left(\frac{\Omega^4}{\Delta_1^4}\right). \tag{S13}$$

Substituting this expansion, we obtain

$$C_2'(t) = \left(1 + \frac{\Omega^2}{\Delta_1^2} + \mathcal{O}\left(\frac{\Omega^4}{\Delta_1^4}\right)\right)\left[\frac{\sqrt{6}A_p}{2\Delta_1}C_1'(t) + \frac{\sqrt{6}A_p\Omega}{2\Delta_1^2}C_{e_1,e_2}(t)\right]. \tag{S14}$$

The term proportional to Ω^2/Δ_1^2 generates corrections of order $\mathcal{O}(A_p\Omega^3/\Delta_1^4)$ and $\mathcal{O}(A_p^2\Omega^2/\Delta_1^4)$. Since our perturbative treatment retains terms only up to second order in the small parameters A_p/Δ_1 and Ω/Δ_1, these higher-order contributions are neglected. As a result,

$$C_2'(t) \simeq \frac{\sqrt{6}A_p}{2\Delta_1}C_1'(t) + \frac{\sqrt{6}A_p\Omega}{2\Delta_1^2}C_{e_1,e_2}(t). \tag{S15}$$

Note: The slowly varying amplitude $C_{e_1,e_2}(t)$ is also assumed to be of order unity, i.e., $C_{e_1,e_2}(t) = \mathcal{O}(1)$. This is justified by our numerical simulations, which show that as the small parameter A_p/Δ_1 is decreased, the maximum value attained by $C_{e_1,e_2}(t)$ remains approximately unchanged (see Fig 4b and 4c in the manuscript). Thus, $C_{e_1,e_2}(t)$ does not scale with A_p/Δ_1 and should be regarded as an $\mathcal{O}(1)$ quantity. Since $C_1'(t)$ is of first order, $C_2'(t)$ is of second order in the small parameters A_p/Δ_1 and Ω/Δ_1.
Now substitute this $C_2'(t)$ into the $C_3'(t)$ we get,

$$C_3'(t) \approx \sqrt{2}\frac{\Omega}{\Delta_1}(\sqrt{3/2}\frac{A_p}{\Delta_1}C_1'(t) + \sqrt{3/2}\frac{A_p\Omega}{\Delta_1^2}C_{e_1,e_2}(t)) + \frac{A_p\sqrt{3}}{\Delta_1}C_{e_1,e_2}(t) \tag{S16}$$

Now, according to the rule we have defined above, the first term is neglected because $C_1'(t)$ is of the order $\mathcal{O}(A_p/\Delta_1)$. As a result, the product $(A_p\Omega/\Delta_1^2)C_1'(t)$ is of order $\mathcal{O}(A_p^2\Omega/\Delta_1^3)$, which is a third-order contribution. The second term is neglected because it is explicitly proportional to $A_p\Omega^2/\Delta_1^3$, which is also of third order. Since our perturbative treatment retains terms only up to second order in the small parameters A_p/Δ_1 and Ω/Δ_1, both terms are neglected. As a result, we get,

$$C_3'(t) \approx \frac{A_p\sqrt{3}}{\Delta_1}C_{e_1,e_2}(t) \tag{S17}$$

Finally, we obtain the quasi-steady-state expression for $C_3'(t)$ solely in terms of the slowly varying amplitude $C_{e_1,e_2}(t)$. After substituting this expression into the differential equation for $C_{e_1,e_2}(t)$

$$i\frac{\partial C_{e_1,e_2}}{\partial t} = \Omega C_1'(t) + A_p\sqrt{3}C_3'(t) \tag{S18}$$

we get,

$$i\frac{\partial C_{e_1,e_2}}{\partial t} \approx \Omega C_1'(t) + \frac{3A_p^2}{\Delta_1}C_{e_1,e_2}(t) \tag{S19}$$

In Eq. S9, the term $\frac{\sqrt{6}A_p}{\Delta_1}C_2'(t)$ is neglected since $C_2'(t)$ is of second order. The additional factor A_p/Δ_1 makes the entire term third order, and it is therefore omitted within our second-order perturbative treatment.

$$C_1'(t) \approx \sqrt{2}\frac{A_p}{\Delta_1}C_{0,g}(t) + \frac{\Omega}{\Delta_1}C_{e_1,e_2}'(t) \tag{S20}$$

Now that we have obtained the quasi-steady state expression for $C_1'(t)$ in terms of the slow variable, we can substitute this expression into the differential equations for $C_{0,g}(t)$ and $C_{e_1,e_2}(t)$:

$$\begin{aligned} i\frac{\partial C_{0,g}}{\partial t} &\approx \sqrt{2}A_p(\sqrt{2}\frac{A_p}{\Delta_1}C_{0,g}(t) + \frac{\Omega}{\Delta_1}C_{e_1,e_2}(t)) \\ i\frac{\partial C_{0,g}}{\partial t} &\approx \frac{2A_p^2}{\Delta_1}C_{0,g}(t) + \frac{\sqrt{2}A_p\Omega}{\Delta_1}C_{e_1,e_2}(t) \end{aligned} \tag{S21}$$

If we substitute Eq.S20 into Eq.S19 we get the differential equation for the C_{e_1,e_2} state:

$$\begin{aligned} i\frac{\partial C_{e_1,e_2}}{\partial t} &\approx \Omega(\sqrt{2}\frac{A_p}{\Delta_1}C_{0,g}(t) + \frac{\Omega}{\Delta_1}C'_{e_1,e_2}(t)) + \frac{3A_p^2}{\Delta_1}C_{e_1,e_2}(t) \\ i\frac{\partial C_{e_1,e_2}}{\partial t} &\approx \frac{\Omega^2+3A_p^2}{\Delta_1}C_{e_1,e_2}(t) + \frac{\sqrt{2}A_p\Omega}{\Delta_1}C_{0,g}(t) \end{aligned} \tag{S22}$$

Putting the above results together, we obtain the effective coupled equations for the slowly varying amplitudes,

$$\begin{aligned} i\frac{\partial C_{0,g}}{\partial t} &\approx \frac{2A_p^2}{\Delta_1}C_{0,g}(t) + \frac{\sqrt{2}A_p\Omega}{\Delta_1}C_{e_1,e_2}(t), \\ i\frac{\partial C_{e_1,e_2}}{\partial t} &\approx \frac{\Omega^2+3A_p^2}{\Delta_1}C_{e_1,e_2}(t) + \frac{\sqrt{2}A_p\Omega}{\Delta_1}C_{0,g}(t). \end{aligned} \tag{S23}$$

Equation (S23) is accurate to second order in the perturbative parameters A_p/Δ_1 and Ω/Δ_1, with all terms of third order and higher consistently neglected.

We compare the populations obtained from the full Hamiltonian in Eq. (S3), numerically solved using `QuTiP`, with those obtained from the effective coupled differential equations in Eq. (S23). We have taken the same value of $A_p = 0.2\Omega$ and $\Delta_1 = 6\Omega$, which are used in the manuscript, so $\Delta_1 = 30A_p$. The maximum population of the state $|\psi_{e_1,e_2}\rangle$ was obtained to be 0.225 for the full numerical simulation, while the coupled differential equation yields 0.228. The error is 0.003 for $\frac{A_p}{\Delta_1} = 0.033$. The close agreement between these values confirms the validity of the adiabatic elimination for the chosen parameter. The period of the oscillation obtained after solving Eq. (S23) is also very close to the value obtained using numerical simulation.

Effective Two-Level Hamiltonian

In this section, we rewrite the coupled differential equations derived in Eq. S23 in a Schrödinger-like form, which allows us to identify the effective Hamiltonian governing the reduced two-state dynamics.

$$i\frac{\partial}{\partial t}\begin{pmatrix} C_{0,g}(t) \\ C_{e_1,e_2}(t) \end{pmatrix} = \hat{H}_{\text{eff}}\begin{pmatrix} C_{0,g}(t) \\ C_{e_1,e_2}(t) \end{pmatrix}, \qquad \begin{pmatrix} C_{0,g}(0) \\ C_{e_1,e_2}(0) \end{pmatrix} = \begin{pmatrix} 1 \\ 0 \end{pmatrix}. \tag{S24}$$

$$\hat{H}_{\text{eff}} = \frac{1}{\Delta_1}\begin{pmatrix} 2A_p^2 & \sqrt{2}A_p\Omega \\ \sqrt{2}A_p\Omega & \Omega^2+3A_p^2 \end{pmatrix}. \tag{S25}$$

The solution for the excited-state amplitude is

$$C_{e_1,e_2}(t) = -i\,\frac{\Omega^e_{\text{eff}}}{\sqrt{(\Omega^e_{\text{eff}})^2+\frac{\delta^2}{4}}}\,e^{-i\frac{(a+d)}{2}t}\,\sin\left(\sqrt{(\Omega^e_{\text{eff}})^2+\frac{\delta^2}{4}}t\right), \tag{S26}$$

where

$$\begin{aligned} a = \frac{2A_p^2}{\Delta_1}, \quad \Omega^e_{\text{eff}} = \frac{\sqrt{2}A_p\Omega}{\Delta_1}, \quad d = \frac{\Omega^2+3A_p^2}{\Delta_1}, \\ \delta = \frac{\Omega^2+3A_p^2}{\Delta_1} - \frac{2A_p^2}{\Delta_1} = \frac{\Omega^2+A_p^2}{\Delta_1} \end{aligned} \tag{S27}$$

The population in the state $|\psi_{e_1,e_2}\rangle$ is therefore

$$|C_{e_1,e_2}(t)|^2 = \frac{(\Omega^e_{\text{eff}})^2}{(\Omega^e_{\text{eff}})^2 + \frac{\delta^2}{4}} \sin^2(\sqrt{(\Omega^e_{\text{eff}})^2 + \frac{\delta^2}{4}} t), \tag{S28}$$

and finally

$$|C_{e_1,e_2}(t)|^2 = \frac{8A_p^2\Omega^2}{A_p^4 + 10A_p^2\Omega^2 + \Omega^4} \sin^2\left(\frac{t}{2\Delta_1}\sqrt{A_p^2 + 10A_p^2\Omega^2 + \Omega^4}\right) \tag{S29}$$

The population oscillates with the generalized Rabi frequency

$$\Omega_R = \frac{1}{2\Delta_1}\sqrt{A_p^4 + 10A_p^2\Omega^2 + \Omega^4}, \tag{S30}$$

and therefore the oscillation period is

$$T = \frac{\pi}{\Omega_R} = \frac{2\pi\Delta_1}{\sqrt{A_p^4 + 10A_p^2\Omega^2 + \Omega^4}}. \tag{S31}$$

The period of oscillation T is directly proportional to Δ_1, implying the larger the detuning in the system, the longer it takes for the population to move from the vacuum into the state $|\psi_{e_1,e_2}\rangle$, it happens because the PDC process and atom-coupling process becomes more inefficient as we increase the value of Δ_1. Further, the expression also shows that for a fixed value of Δ_1, increasing the value of A_p shortens the period of oscillation. Remember, this expression is only valid under the adiabatic regime.

S3. DETERMINISTIC GENERATION OF THE STATE $|\psi_{e_1,e_2}\rangle$ BY INTRODUCING PHASE CHANGE IN THE PUMP FIELD

The difficulty in achieving deterministic population transfer to the state $|\psi_{e_1,e_2}\rangle$ can be overcome by applying a controlled time-dependent phase modulation to the pump field. To illustrate this protocol explicitly, we consider phase profiles consisting of two sequential π phase flips, as shown in Fig. S1. This is the same pump-field phase profile engineered to generate the state $|\psi_{e_1,e_2}\rangle$ with unit probability in Fig. 5 of the manuscript. Each phase flip corresponds to a rapid transformation $A_p \to -A_p$, implemented using a smooth hyperbolic tangent function. The time-dependent

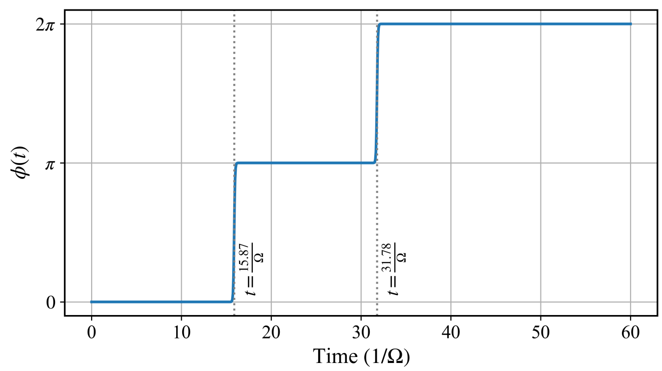

Figure S1: Time-dependent phase profile of the pump field illustrating two controlled π phase flips used to engineer constructive interference in the system dynamics. This phase profile with $\sigma = 0.1\Omega$ is employed to achieve near-deterministic generation of the state $|\psi_{e_1,e_2}\rangle$ in Fig. 5 of the manuscript.

phase modulation of the pump field is modeled as

$$\theta(t) = \sum_{j=1}^{N} \pi \, \frac{1 + \tanh\left(\dfrac{t - t_j}{\sigma}\right)}{2}, \tag{S32}$$

where t_j denotes the time of the j-th phase flip and σ determines how fast the phase change has been implemented. The corresponding effective nonlinear coupling strength is therefore written as

$$A_p(t) = A_p e^{-i\theta(t)}. \tag{S33}$$

Figure S2a(a) shows the maximum probability $P_{\max}$ of the target state $|\psi_{e_1,e_2}\rangle$ as a function of the nonlinear coupling strength A_p/Ω and detuning Δ_1/Ω ($\Delta_1 = \Delta_2$). The integers overlaid on the heatmap indicate the number of phase flips required to reach the corresponding maximum probability. For $A_p \lesssim 0.25$, two phase flips are required to reach the near-deterministic regime. In contrast, for $0.36 \lesssim A_p \lesssim 0.5$, a single phase flip is sufficient to achieve a near-deterministic generation probability. For larger values of A_p and smaller values of Δ_1, the behavior becomes irregular: in some regions, up to three phase flips are required, and the maximum achievable probability is generally reduced. This is reflected in the non-smooth structure of the heatmap in this parameter regime. The irregular features observed at larger A_p and smaller Δ_1 can be attributed to the breakdown of the adiabatic approximation, where the higher-order states play a role in the dynamics and can not be neglected.

There exist parameter regimes in which the system remains in the adiabatic regime, yet the application of phase flips does not lead to near-deterministic generation probability of $|\psi_{e_1,e_2}\rangle$. Thus, the effectiveness of the phase-flip protocol depends on the value of A_p/Ω even within the adiabatic regime. For smaller values of $A_p \lesssim 0.25$, the first maximum is relatively low (e.g., for $A_p = 0.2\Omega$ and $\Delta_1 = 6\Omega$, $P_{\max} \approx 0.22$), and a single phase flip is insufficient to reach the near-deterministic regime. In this case, successive phase flips enhance constructive interference, allowing the probability to gradually approach unity. In contrast, for $0.38\Omega \lesssim A_p \lesssim 0.5\Omega$, the first maximum is already sufficiently large such that a single phase flip drives the system into the near-deterministic regime. A different behavior is observed for $0.25\Omega \lesssim A_p \lesssim 0.38\Omega$. In this regime, one or two phase flips increase the target-state probability to above 0.90, but the probability remains well below the near-deterministic regime. Subsequent phase flips produce no appreciable increase in the generation probability of $|\psi_{e_1,e_2}\rangle$, indicating that the protocol has reached its maximum achievable probability for these parameters. A similar saturation is also observed for larger values of A_p within the adiabatic regime. Here, the first maximum is already high (typically $P \gtrsim 0.5$), and a single phase flip brings the system close

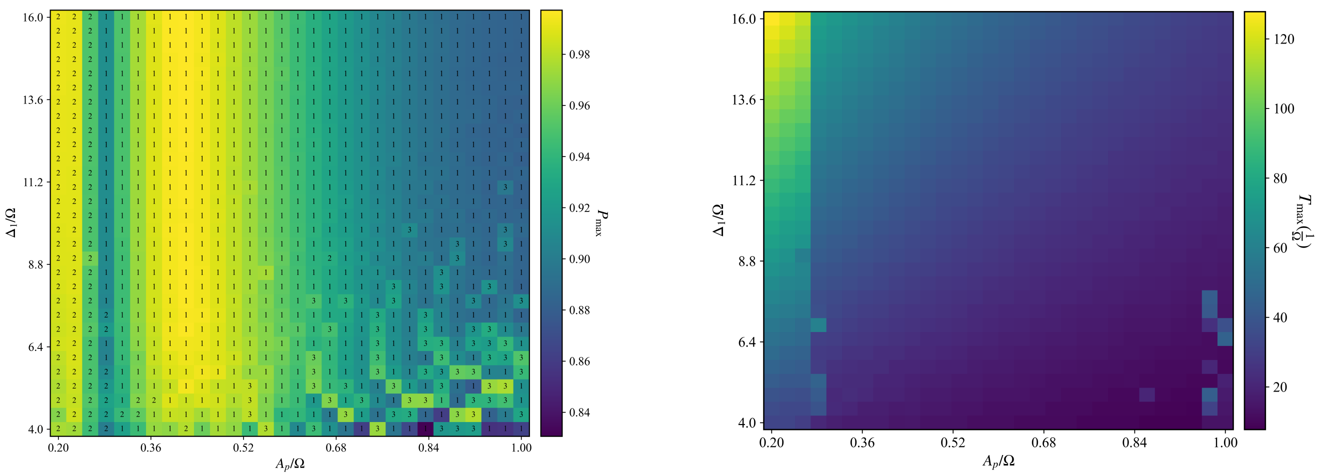

(a) (b)

Figure S2: (a) Maximum probability of generating the state $|\psi_{e_1,e_2}\rangle$ as a function of Δ_1 and A_p. The integers overlaid on the heatmap indicate the number of phase flips required to reach the corresponding maximum probability. (b) Time required for the $|\psi_{e_1,e_2}\rangle$ state to reach its maximum probability when the pump amplitude is modulated as $A_p e^{-i\theta(t)}$.

to its maximal achievable population (see Fig. S2a). As a result, additional phase flips do not significantly improve the generation probability.

These observations indicate that the present protocol, where phase flips are applied precisely at the population maxima with a fixed transition width, is not necessarily optimal. Improved performance may be achieved by applying the phase shifts at earlier times, before the population reaches its maximum, or by tuning the width of the phase-flip transition to better match the system dynamics.

Figure S2b shows the corresponding time $T_{\max}$ required to reach the maximum population. As expected, $T_{\max}$ decreases with increasing A_p, reflecting the increase in the effective coupling strength. However, for small A_p, the timescale becomes significantly larger, consistent with the slower dynamics in the weak-driving regime.

S4. COUPLED DIFFERENTIAL EQUATION B/W VACUUM STATE $|0\rangle$ AND THE STATE $|\psi_{m_1,m_2}\rangle$ OBTAINED AFTER ADIABATIC ELIMINATION

In this section, we derive the differential Eq. (2) in the manuscript, describing the evolution of the state $|0,0,0,0,g\rangle \equiv |0;g\rangle$ and the atom-photon entangled state $|\psi_{m_1,m_2}\rangle$. The Hamiltonian of the system is:

$$\begin{aligned}\hat{H}(t) &= \hat{H}_{NL}(t) + \hat{H}_{e\leftrightarrow g}(t) + \hat{H}_{e\leftrightarrow m}(t)\\ \hat{H}(t) &= \hbar A_p\left[\hat{a}_L^\dagger\hat{b}_R^\dagger + \hat{a}_R^\dagger\hat{b}_L^\dagger\right]e^{-i\Delta_1 t} + \hbar\Omega\left[\hat{a}_L\left|e_1\right\rangle\left\langle g\right| - \hat{a}_R\left|e_2\right\rangle\left\langle g\right|\right]e^{i\Delta_2 t} + \hbar A_c\left[\left|e_1\right\rangle\left\langle m_1\right| + \left|e_2\right\rangle\left\langle m_2\right|\right]e^{i\Delta_3 t} + \text{H.c}\end{aligned} \tag{S34}$$

We will take an ansatz for our $|\psi\rangle$ at any time t as:

$$|\psi(t)\rangle = C_{0,g}(t)\,|0;g\rangle + C_1(t)\,|\phi_1;g\rangle + C_2(t)\,|\phi_2;g\rangle + C_{e_1,e_2}(t)\,|\psi_{e_1,e_2}\rangle + C_3(t)\,|\psi_1\rangle + C_{m_1,m_2}(t)\,|\psi_{m_1,m_2}\rangle + C_4(t)\,|\psi_2\rangle \tag{S35}$$

All the states are the same as described in the manuscript and in the previous section (see Eq.S5). The new state $|\psi_2\rangle$ is: $|\psi_2\rangle = \sqrt{\frac{1}{3}}(|1,0,0,2,m_1\rangle - |0,1,2,0,m_2\rangle) + \frac{1}{\sqrt{6}}(|0,1,1,1,m_1\rangle - |1,0,1,1,m_2\rangle)$. Following the same argument as in Sec. S2, we have neglected higher-order states since their impact is negligible in the regime $A_p \ll \Delta_1$. The differential equations for the amplitudes are:

$$\begin{aligned}i\frac{\partial C_{0,g}}{\partial t} &= \sqrt{2}A_p e^{i\Delta_1 t}C_1(t)\\ i\frac{\partial C_1}{\partial t} &= \sqrt{2}A_p e^{-i\Delta_1 t}C_{0,g}(t) + \sqrt{6}A_p e^{i\Delta_1 t}C_2(t) + \Omega C_{e_1,e_2}(t)e^{-i\Delta_2 t}\\ i\frac{\partial C_2}{\partial t} &= \sqrt{6}A_p e^{-i\Delta_1 t}C_1(t) + \sqrt{2}\Omega C_3(t)e^{-i\Delta_2 t}\\ i\frac{\partial C_{e_1,e_2}}{\partial t} &= \Omega e^{i\Delta_2 t}C_1(t) + A_p\sqrt{3}C_3(t)e^{i\Delta_1 t} + A_c C_{m_1,m_2}(t)e^{i\Delta_3 t}\\ i\frac{\partial C_3}{\partial t} &= \sqrt{2}\Omega C_2(t)e^{i\Delta_2 t} + A_p\sqrt{3}C_{e_1,e_2}(t)e^{-i\Delta_1 t} + A_c C_4(t)e^{i\Delta_3 t}\\ i\frac{\partial C_{m_1,m_2}}{\partial t} &= A_c C_{e_1,e_2}(t)e^{-i\Delta_3 t} + A_p\sqrt{3}C_4(t)e^{i\Delta_1 t}\\ i\frac{\partial C_4}{\partial t} &= A_c C_3(t)e^{-i\Delta_3 t} + A_p\sqrt{3}C_{m_1,m_2}(t)e^{-i\Delta_1 t}\end{aligned} \tag{S36}$$

Here, we will again transform the amplitudes in the rotating frame picture to remove the fast exponentially oscillating terms. $C_1'(t) = C_1(t)e^{i\Delta_1 t}, C_2'(t) = C_2(t)e^{i2\Delta_1 t}, C_{e_1,e_2}'(t) = e^{i(\Delta_1-\Delta_2)t}C_{e_1,e_2}(t)$ and $C_3'(t) = e^{i(2\Delta_1-\Delta_2)t}C_3(t), C_{m_1,m_2}'(t) = e^{i(\Delta_1-\Delta_2+\Delta_3)t}C_{m_1,m_2}(t)$ and $C_4'(t) = e^{i(2\Delta_1-\Delta_2+\Delta_3)t}C_4(t)$. The differential equation after removing the fast-oscillating terms is:

$$\begin{aligned}i\frac{\partial C_{0,g}}{\partial t} &= \sqrt{2}A_p C_1'(t)\\ i\frac{\partial C_1'}{\partial t} &= -\Delta_1 C_1'(t) + \sqrt{2}A_p C_{0,g}(t) + \sqrt{6}A_p C_2'(t) + \Omega C_{e_1,e_2}'(t)\\ i\frac{\partial C_2'}{\partial t} &= -2\Delta_1 C_2'(t) + \sqrt{6}A_p C_1'(t) + \sqrt{2}\Omega C_3'(t)\\ i\frac{\partial C_{e_1,e_2}'}{\partial t} &= -(\Delta_1-\Delta_2)C_{e_1,e_2}' + \Omega C_1'(t) + A_p\sqrt{3}C_3'(t) + A_c C_{m_1,m_2}'(t)\\ i\frac{\partial C_3'}{\partial t} &= -(2\Delta_1-\Delta_2)C_3'(t) + \sqrt{2}\Omega C_2'(t) + A_p\sqrt{3}C_{e_1,e_2}'(t) + A_c C_4'(t)\\ i\frac{\partial C_{m_1,m_2}'}{\partial t} &= -(\Delta_1-\Delta_2+\Delta_3)C_{m_1,m_2}'(t) + A_c C_{e_1,e_2}'(t) + A_p\sqrt{3}C_4'(t)\\ i\frac{\partial C_4'}{\partial t} &= -(2\Delta_1-\Delta_2+\Delta_3)C_4' + A_c C_3'(t) + A_p\sqrt{3}C_{m_1,m_2}'(t)\end{aligned} \tag{S37}$$

Now, we impose the resonance condition $\Delta_1 + \Delta_3 = \Delta_2$ and assume the large-detuning regime, where Δ_1, Δ_3, and $|\Delta_1 - \Delta_3|$ are all much larger than A_p, Ω, and A_c. After imposing this condition, we can categorize the probability amplitude $C_{0,g}(t)$ and $C_{m_1,m_2}(t)$ as slow variables and others as fast variables. As a result, the fast variables can be adiabatically eliminated from the dynamics, and the complete description of the system can be reduced to an effective coupled differential equation between the vacuum and the light-matter entangled state $|\psi_{m_1,m_2}\rangle$. Let us repeat the procedure for adiabatically eliminating the fast variables by first setting their derivatives to zero. Note: when we impose the condition $\Delta_1+\Delta_3=\Delta_2$ we get $C'_{m_1,m_2}(t)=C_{m_1,m_2}(t)$.

$$\begin{aligned}
i\frac{\partial C_{0,g}}{\partial t} &= \sqrt{2}A_pC'_1(t)\\
0 &= -\Delta_1C'_1(t)+\sqrt{2}A_pC_{0,g}(t)+\sqrt{6}A_pC'_2(t)+\Omega C'_{e_1,e_2}(t)\\
0 &= -2\Delta_1C'_2(t)+\sqrt{6}A_pC'_1(t)+\sqrt{2}\Omega C'_3(t)\\
0 &= \Delta_3C'_{e_1,e_2}+\Omega C'_1(t)+A_p\sqrt{3}C'_3(t)+A_cC'_{m_1,m_2}(t)\\
0 &= -(\Delta_1-\Delta_3)C'_3(t)+\sqrt{2}\Omega C'_2(t)+A_p\sqrt{3}C'_{e_1,e_2}(t)+A_cC'_4(t)\\
i\frac{\partial C_{m_1,m_2}}{\partial t} &= A_cC'_{e_1,e_2}(t)+A_p\sqrt{3}C'_4(t)\\
0 &= -\Delta_1C'_4+A_cC'_3(t)+A_p\sqrt{3}C'_{m_1,m_2}(t)
\end{aligned} \tag{S38}$$

Although the derivation below assumes Δ_1, Δ_3, and $|\Delta_1-\Delta_3|$ are much larger than A_p, Ω, and A_c, our numerical simulations indicate that the perturbative treatment remains accurate even when $\Delta_1=\Delta_3$. This suggests that the condition $|\Delta_1-\Delta_3|\gg A_p,\Omega,A_c$ is sufficient but not necessary for the validity of the adiabatic elimination in the parameter regime considered.
Let us write an expression for the quasi-steady-state value of $C'_4(t)$:

$$C'_4(t)=\frac{A_c}{\Delta_1}\,C'_3(t)+\frac{\sqrt{3}\,A_p}{\Delta_1}\,C_{m_1,m_2}(t). \tag{S39}$$

As in the previous section, the same perturbative order is employed throughout this derivation. In particular, $C_{0,g}(t)$ and $C'_{m_1,m_2}(t)$ are treated as quantities of order unity, and terms of order $\left(\frac{A_p,\Omega,A_c}{\Delta}\right)^3$ and higher are neglected. Insert Eq. (S39) into quasi steady state equation for $C'_3(t)$:

$$\left(\Delta_1-\Delta_3-\frac{A_c^2}{\Delta_1}\right)C'_3(t)=\sqrt{2}\Omega C'_2(t)+\sqrt{3}A_pC'_{e_1,e_2}(t)+\frac{\sqrt{3}A_pA_c}{\Delta_1}C'_{m_1,m_2}(t). \tag{S40}$$

The inverse prefactor is expanded perturbatively as

$$\frac{1}{\Delta_1-\Delta_3-\frac{A_c^2}{\Delta_1}}=\frac{1}{\Delta_1-\Delta_3}\left[1+\frac{A_c^2}{\Delta_1(\Delta_1-\Delta_3)}+\mathcal{O}\left(\frac{A_c^4}{\Delta_1^2(\Delta_1-\Delta_3)^2}\right)\right]. \tag{S41}$$

Since the correction proportional to A_c^2 generates third- and higher-order contributions when multiplied by the terms on the right-hand side, it is neglected within our second-order perturbative treatment. Therefore,

$$C'_3(t)\approx\frac{\sqrt{2}\Omega}{(\Delta_1-\Delta_3)}C'_2(t)+\frac{\sqrt{3}A_p}{(\Delta_1-\Delta_3)}C'_{e_1,e_2}(t)+\frac{\sqrt{3}\,A_cA_p}{(\Delta_1-\Delta_3)\Delta_1}C_{m_1,m_2}(t) \tag{S42}$$

From the above expression, $C'_3(t)$ is of second order, i.e., $C'_3(t)=\mathcal{O}\left(\left(\frac{A_p,\Omega,A_c}{\Delta}\right)^2\right)$, since its leading contribution is proportional to $\frac{A_pA_c}{\Delta^2}C'_{m_1,m_2}(t)$, where $C'_{m_1,m_2}(t)$ is of order unity. Since $C'_3(t)$ is a second-order quantity, the term $\frac{A_c}{\Delta_1}C'_3(t)$ in the expression for $C'_4(t)$ (Eq.S39) is third order and can be neglected within our second-order perturbative treatment. Thus, the quasi steady state value of $C'_4(t)$ now approximate to:

$$C'_4(t)\approx\frac{\sqrt{3}\,A_p}{\Delta_1}\,C_{m_1,m_2}(t). \tag{S43}$$

The steady state expression of $C'_{e_1,e_2}(t)$ is:

$$C'_{e_1,e_2}=-\frac{\Omega}{\Delta_3}C'_1(t)-\frac{A_p\sqrt{3}}{\Delta_3}C'_3(t)-\frac{A_c}{\Delta_3}C'_{m_1,m_2}(t) \tag{S44}$$

Since the order of $C_3'(t)$ is of second order, the term $\frac{A_p\sqrt{3}}{\Delta_3}C_3'(t)$ can be dropped since it is a term of third order.

$$C'_{e_1,e_2} \approx -\frac{\Omega}{\Delta_3}C_1'(t) - \frac{A_c}{\Delta_3}C'_{m_1,m_2}(t) \tag{S45}$$

From the above expression we can deduce that C'_{e_1,e_2} is of first order, i.e., $C'_{e_1,e_2}(t) = \mathcal{O}\left(\frac{A_c}{\Delta_3}\right)$. The quasi-steady value for $C_2'(t)$ is

$$C_2'(t) = \frac{\sqrt{6}A_p}{2\Delta_1}C_1'(t) + \frac{\sqrt{2}\Omega}{2\Delta_1}C_3'(t). \tag{S46}$$

Again we can neglect the term $\frac{\sqrt{2}\Omega}{2\Delta_1}C_3'(t)$ from the above expression resulting in:

$$C_2'(t) \approx \frac{\sqrt{6}}{2}\frac{A_p}{\Delta_1}C_1'(t) \tag{S47}$$

Finally we write the quasi-steady-state value of C_1':

$$C_1'(t) = \sqrt{2}\frac{A_p}{\Delta_1}C_{0,g}(t) + \sqrt{6}\frac{A_p}{\Delta_1}C_2'(t) + \frac{\Omega}{\Delta_1}C'_{e_1,e_2}(t) \tag{S48}$$

$$\begin{aligned} C_1'(t) &= \sqrt{2}\frac{A_p}{\Delta_1}C_{0,g}(t) + \sqrt{6}\frac{A_p}{\Delta_1}\left(\frac{\sqrt{6}A_p}{2\Delta_1}C_1'(t)\right) + \frac{\Omega}{\Delta_1}C'_{e_1,e_2}(t) \\ &= \sqrt{2}\frac{A_p}{\Delta_1}C_{0,g}(t) + 3\frac{A_p^2}{\Delta_1^2}C_1'(t) + \frac{\Omega}{\Delta_1}C'_{e_1,e_2}(t). \end{aligned} \tag{S49}$$

Further we substitute the value of Eq. S45 into the Eq. S53 we get:

$$\begin{aligned} C_1'(t) &= \sqrt{2}\frac{A_p}{\Delta_1}C_{0,g}(t) + 3\frac{A_p^2}{\Delta_1^2}C_1'(t) - \frac{\Omega}{\Delta_1}\left[\frac{\Omega}{\Delta_3}C_1'(t) + \frac{A_c}{\Delta_3}C'_{m_1,m_2}(t)\right] \\ &= \sqrt{2}\frac{A_p}{\Delta_1}C_{0,g}(t) + \left(3\frac{A_p^2}{\Delta_1^2} - \frac{\Omega^2}{\Delta_1\Delta_3}\right)C_1'(t) - \frac{\Omega A_c}{\Delta_1\Delta_3}C'_{m_1,m_2}(t). \end{aligned} \tag{S50}$$

$$\left[1 - 3\frac{A_p^2}{\Delta_1^2} + \frac{\Omega^2}{\Delta_1\Delta_3}\right]C_1'(t) = \sqrt{2}\frac{A_p}{\Delta_1}C_{0,g}(t) - \frac{\Omega A_c}{\Delta_1\Delta_3}C'_{m_1,m_2}(t). \tag{S51}$$

$$\begin{aligned} C_1'(t) &= \frac{\sqrt{2}\frac{A_p}{\Delta_1}C_{0,g}(t) - \frac{\Omega A_c}{\Delta_1\Delta_3}C'_{m_1,m_2}(t)}{1 - \left(3\frac{A_p^2}{\Delta_1^2} - \frac{\Omega^2}{\Delta_1\Delta_3}\right)} \\ &\approx \left[1 + 3\frac{A_p^2}{\Delta_1^2} - \frac{\Omega^2}{\Delta_1\Delta_3}\right]\left[\sqrt{2}\frac{A_p}{\Delta_1}C_{0,g}(t) - \frac{\Omega A_c}{\Delta_1\Delta_3}C'_{m_1,m_2}(t)\right]. \end{aligned} \tag{S52}$$

Since the correction factor in the square brackets is already of second order, its product with the first term on the right-hand side generates third-order contributions, while its product with the second term generates fourth-order contributions. Therefore, within our second-order perturbative treatment, these higher-order terms are neglected, resulting

$$C_1'(t) \approx \sqrt{2}\frac{A_p}{\Delta_1}C_{0,g}(t) - \frac{\Omega A_c}{\Delta_1\Delta_3}C'_{m_1,m_2}(t). \tag{S53}$$

The amplitude $C_1'(t)$ is of first order i.e., $\mathcal{O}(\frac{A_p}{\Delta_1})$. Finally, we insert the value of $C_1'(t)$ from Eq. S53 into the differential equation for the vacuum state $|0;g\rangle$:

$$\begin{aligned} i\frac{\partial C_{0,g}}{\partial t} &\approx \sqrt{2}A_p(\sqrt{2}\frac{A_p}{\Delta_1}C_{0,g}(t) - \frac{\Omega A_c}{\Delta_1\Delta_3}C_{m_1,m_2}(t)) \\ i\frac{\partial C_{0,g}}{\partial t} &\approx \frac{2A_p^2}{\Delta_1}C_{0,g}(t) - \frac{\sqrt{2}A_p\Omega A_c}{\Delta_1\Delta_3}C_{m_1,m_2}(t) \end{aligned} \tag{S54}$$

Now, to obtain the differential equation for $C'_{m_1,m_2}(t)$ in terms of slow variables, we substitute Eq.S43 and Eq.S45 into the differential equation for C_{m_1,m_2}:

$$\begin{aligned} i\frac{\partial C_{m_1,m_2}}{\partial t} &\approx -A_c(\frac{\Omega}{\Delta_3}C'_1(t)+\frac{A_c}{\Delta_3}C'_{m_1,m_2}(t))+A_p\sqrt{3}(\frac{\sqrt{3}\,A_p}{\Delta_1}\,C_{m_1,m_2}(t)) \\ i\frac{\partial C_{m_1,m_2}}{\partial t} &\approx -\frac{A_c\Omega}{\Delta_3}C'_1(t)+(-\frac{A_c^2}{\Delta_3}+\frac{3A_p^2}{\Delta_1})C_{m_1,m_2}(t) \end{aligned} \tag{S55}$$

Now, we insert the value of $C'_1(t)$ from the Eq. S53, and then neglecting the terms of the order $\mathcal{O}(\frac{A}{\Delta})^3$ we get,

$$i\frac{\partial C_{m_1,m_2}}{\partial t} \approx (\frac{3A_p^2}{\Delta_1}-\frac{A_c^2}{\Delta_3})C_{m_1,m_2}(t)-\frac{\sqrt{2}A_pA_c\Omega}{\Delta_1\Delta_3}C_{0,g}(t) \tag{S56}$$

Putting the two differential equations together, we get,

$$\begin{aligned} i\frac{\partial C_{0,g}}{\partial t} &\approx \frac{2A_p^2}{\Delta_1}C_{0,g}(t)-\frac{\sqrt{2}A_pA_c\Omega}{\Delta_1\Delta_3}C_{m_1,m_2}(t), \\ i\frac{\partial C_{m_1,m_2}}{\partial t} &\approx \left(\frac{3A_p^2}{\Delta_1}-\frac{A_c^2}{\Delta_3}\right)C_{m_1,m_2}(t)-\frac{\sqrt{2}A_pA_c\Omega}{\Delta_1\Delta_3}C_{0,g}(t). \end{aligned} \tag{S57}$$

Although the above derivation assumes $|\Delta_1-\Delta_3| \gg A_p,\Omega,A_c$, our numerical simulations show that the effective two-state description remains accurate even when

$$\Delta_1 = \Delta_3.$$

This indicates that the condition $|\Delta_1-\Delta_3| \gg A_p,\Omega,A_c$ is sufficient but not necessary for the validity of the adiabatic elimination in the parameter regime considered. This is because $C'_3(t)$, which is the only amplitude whose quasi-steady-state expression explicitly depends on the condition $|\Delta_1-\Delta_3| \gg A_p,\Omega,A_c$, is itself a second-order quantity. Moreover, whenever $C'_3(t)$ is substituted into the remaining probability amplitudes, its contribution appears only at third and higher orders in the perturbative expansion. As a result, its effect on the relevant probability amplitudes is negligible within the second-order perturbative treatment adopted here.

On solving the above differential equation, we obtain the probability amplitude for the $C_{m_1,m_2}(t)$ as:

$$C_{m_1,m_2}(t) = i\,\frac{\Omega^m_{\text{eff}}}{\Omega_T}\,e^{-i(a+d)t/2}\sin(\Omega_T t), \tag{S58}$$

where

$$a=\frac{2A_p^2}{\Delta_1}, \qquad \Omega^m_{\text{eff}}=\frac{\sqrt{2}\,A_pA_c\Omega}{\Delta_1\Delta_3}, \qquad d=\frac{3A_p^2}{\Delta_1}-\frac{A_c^2}{\Delta_3}, \qquad \delta_m=d-a=\frac{A_p^2}{\Delta_1}-\frac{A_c^2}{\Delta_3} \tag{S59}$$

and

$$\Omega_{\text{T}}=\sqrt{\delta_m^2+(\Omega^m_{\text{eff}})^2}=\sqrt{\frac{2A_p^2A_c^2\Omega^2}{\Delta_1^2\Delta_3^2}+\frac{1}{4}\left(\frac{A_c^2}{\Delta_3}-\frac{A_p^2}{\Delta_1}\right)^2}. \tag{S60}$$

Hence,

$$C_{m_1,m_2}(t)=i\,\frac{\dfrac{\sqrt{2}\,A_pA_c\Omega}{\Delta_1\Delta_3}}{\sqrt{\dfrac{2A_p^2A_c^2\Omega^2}{\Delta_1^2\Delta_3^2}+\dfrac{1}{4}\left(\dfrac{A_c^2}{\Delta_3}-\dfrac{A_p^2}{\Delta_1}\right)^2}}\,e^{-i\left(\frac{5A_p^2}{2\Delta_1}-\frac{A_c^2}{2\Delta_3}\right)t}\sin\left[t\sqrt{\frac{2A_p^2A_c^2\Omega^2}{\Delta_1^2\Delta_3^2}+\frac{1}{4}\left(\frac{A_c^2}{\Delta_3}-\frac{A_p^2}{\Delta_1}\right)^2}\right]. \tag{S61}$$

S5. COUPLING STRENGTH Ω AND A_c

A. The Case for $\Omega_1 = -\Omega_2$

The multilevel atom considered in this work can be physically realized using a single ^{87}Rb atom. The atom is prepared in the ground hyperfine state $|g\rangle = |F{=}1, m_F{=}0\rangle$ of the $5\,^2S_{1/2}$ manifold ($J{=}1/2$, $L{=}0$), excited on the D_2 line ($5\,^2S_{1/2} \rightarrow 5\,^2P_{3/2}$) to the hyperfine levels $|e_{1 \text{ or } 2}\rangle = |F'{=}1, m'_F{=}\pm1\rangle$ using LHC and RHC-polarized light. The coupling strength Ω is defined as:

$$\begin{aligned}\Omega_1 &= \frac{\mathbf{d}_{|e_1\rangle\leftrightarrow|g\rangle}.\mathbf{E_i^L}(\mathbf{r})}{\hbar} \\ \Omega_2 &= \frac{\mathbf{d}_{|e_2\rangle\leftrightarrow|g\rangle}.\mathbf{E_i^R}(\mathbf{r})}{\hbar}\end{aligned} \tag{S62}$$

$\mathbf{E_i^L}(\mathbf{r})$ and $\mathbf{E_i^R}(\mathbf{r})$ are the Electric field profiles of the idler modes of the cavity for Left and Right circular polarizations. The circularly polarized idler modes are taken to be frequency-degenerate with the same spatial variation at the atomic position, i.e. $\mathbf{E}_i^L(\mathbf{r}) = \mathcal{E}(\mathbf{r})\,\mathbf{e}_L$ and $\mathbf{E}_i^R(\mathbf{r}) = \mathcal{E}(\mathbf{r})\,\mathbf{e}_R$, where $|\mathcal{E}(\mathbf{r})|$ is identical for both polarizations (up to a controllable global phase). The relevant dipole transitions obey the selection rules $m_F = 0 \rightarrow m'_F = \pm1$, hence $\mathbf{d}_{|e_1\rangle\leftrightarrow|g\rangle} \propto \mathbf{e}_L$ and $\mathbf{d}_{|e_2\rangle\leftrightarrow|g\rangle} \propto \mathbf{e}_R$, so that $\mathbf{d}_{|e_1\rangle\leftrightarrow|g\rangle} \cdot \mathbf{E}_i^L \propto d_L\mathcal{E}(\mathbf{r})$ and $\mathbf{d}_{|e_2\rangle\leftrightarrow|g\rangle} \cdot \mathbf{E}_i^R \propto d_R\mathcal{E}(\mathbf{r})$. For the symmetric pair of transitions the Clebsch-Gordan coefficients satisfy $|d_L| = |d_R|$ with opposite sign, which leads to $\Omega_1 = -\Omega_2$ [S2].

B. The case for equal coupling strength for the processes $|e_1\rangle \leftrightarrow |m_1\rangle$ and $|e_2\rangle \leftrightarrow |m_2\rangle$

The atom is driven by a π-polarized control field that couples the excited states $|e_{1,2}\rangle = |F' = 1, m'_F = \pm1\rangle$ to the long-lived hyperfine states $|m_{1,2}\rangle = |F = 2, m_F = \pm1\rangle$. The corresponding coupling strengths are

$$\begin{aligned}A_c^1 &= \frac{\mathbf{d}_{e_1\leftrightarrow m_1} \cdot \mathbf{E}_c(\mathbf{r})}{\hbar}, \\ A_c^2 &= \frac{\mathbf{d}_{e_2\leftrightarrow m_2} \cdot \mathbf{E}_c(\mathbf{r})}{\hbar}.\end{aligned} \tag{S63}$$

Since the control field is π-polarized, it drives only $\Delta m_F = 0$ transitions. Both transitions, therefore, involve the same change in magnetic quantum number, i.e., zero, and connect symmetric Zeeman sublevels ($m_F = \pm1$) within the same hyperfine manifolds. According to the Wigner-Eckart theorem, the reduced dipole matrix for both transitions will be identical since both transitions involve the same $F' = 1$ and $F = 2$ hyperfine levels. The reduced dipole matrix does not depend on magnetic quantum numbers. All the m_F dependencies sit in Clebsch-Gordan coefficients $\langle F' = 1, m'_F;\, 1, 0 \mid F = 2, m_F\rangle$. Clebsch-Gordan coefficients always satisfy $|\langle F' = 1, m'_F = 1;\, 1, 0 \mid F = 2, m_F = 1\rangle| = |\langle F' = 1, m'_F = -1;\, 1, 0 \mid F = 2, m_F = -1\rangle|$, hence the dipole matrix element for both transitions will be equal. Since only π-polarized transitions are possible (preserving the magnetic quantum number), both dipole matrix elements will be parallel to the control field. This implies:

$$A_c^1 = A_c^2 \equiv A_c. \tag{S64}$$

S6. WHY DOES INCREASING A_p EVENTUALLY DEGRADE THE FIDELITY OF GENERATING $|\psi_{m_1,m_2}\rangle$ IN THE CONTINUOUS-WAVE PUMPING REGIME?

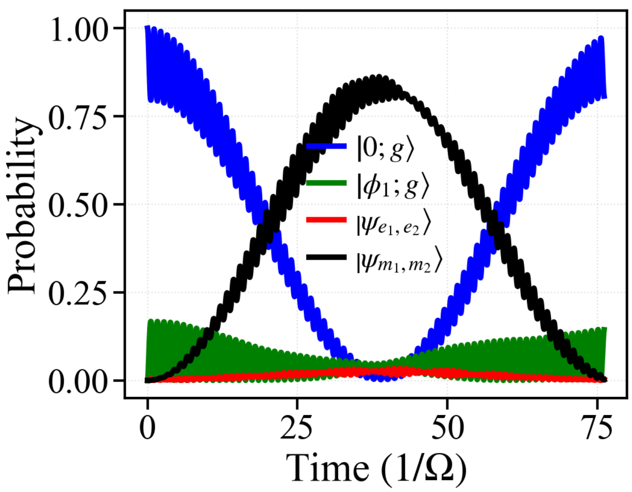

(a) $A_p = \Omega$, $\Delta_1 = 6\Omega = \Delta_3$.

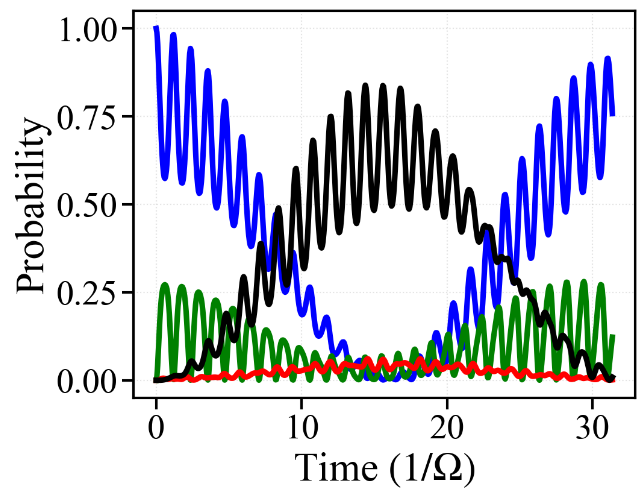

(b) $A_p = 1.5\Omega$, $\Delta_1 = 6\Omega = \Delta_3$.

Figure S3: Temporal evolution of the cavity-atom states for two different pump strengths while $\Delta_1 = \Delta_3 = 6\Omega$.

In Fig. S3, the nonlinear coupling strengths are chosen as $A_p = \Omega$ and $A_p = 1.5\Omega$, which are respectively 5 and 7.5 times larger than the value $A_p = 0.2\Omega$ used in Fig. 6(b) of the manuscript. The values $A_c = 1.05\Omega$ in Fig. S3a and $A_c = 1.7\Omega$ in Fig. S3b were determined numerically such that the vacuum state $|0; g\rangle$ is completely depleted. For these parameter values, the timescale for generating the state $|\psi_{m_1,m_2}\rangle$ is significantly reduced from approximately $1000/\Omega$ in Fig. 6(b) of the manuscript to $38.6/\Omega$ in Fig. S3a and $14.4/\Omega$ in Fig. S3b. However, this speedup comes at the expense of a reduced probability of generation. The maximum probability of generating the state $|\psi_{m_1,m_2}\rangle$ decreases to 0.862 for $A_p = \Omega$ and 0.84 for $A_p = 1.5\Omega$, compared to the near-deterministic generation achieved in Fig. 6(b) of the manuscript. This reduction occurs because the off-resonant intermediate states $|\phi_1; g\rangle$ and $|\psi_{e_1,e_2}\rangle$ acquire finite population, indicating the system is not strictly in an adiabatic regime. Nevertheless, the generation times of $38.6/\Omega$ and $14.4/\Omega$ remain in good agreement with the adiabatic-elimination prediction, $T = \frac{\pi}{2\Omega^m_{\text{eff}}}$, which yields $T = 38.06/\Omega$ for $A_p = \Omega$ and $T = 15.7/\Omega$ for $A_p = 1.5\Omega$, suggesting that the system continues to operate in a quasi-adiabatic regime. Another indication of quasi-adiabatic behavior is that choosing $A_c = \Omega$ from the adiabatic-elimination condition $A_c = A_p\sqrt{\frac{\Delta_3}{\Delta_1}}$, does not maximize the generation probability. Instead, numerical optimization yields $A_c = 1.05\Omega$, for which the maximum probability increases to 0.86, whereas the adiabatic value $A_c = \Omega$ results in a lower probability of 0.78. This deviation from the adiabatic prediction further supports the interpretation that the system operates in a quasi-adiabatic regime. Likewise, for $A_p = 1.5\Omega$, the adiabatic prediction is $A_c = 1.5\Omega$, whereas the optimal value shifts further to $A_c = 1.7\Omega$. The increasing deviation of the A_c from the adiabatic prediction as A_p increases indicates that the system gradually moves farther away from the ideal adiabatic regime, while still retaining the essential characteristics of quasi-adiabatic dynamics. In the continuous-wave (CW) regime, there exists a trade-off between generation efficiency and generation time. Achieving deterministic generation of the state $|\psi_{m_1,m_2}\rangle$ requires operating in the adiabatic regime, which necessitates $A_p \ll \Delta_1$. While this condition suppresses off-resonant intermediate-state populations and enables complete population transfer, it also reduces the effective coupling strength, thereby increasing the generation time.

S7. PDC PROCESS USING A PUMP PULSE UNDER OFF-RESONANT DRIVING

In this section, we will describe the PDC process by operating the pump in the pulse mode. The detunings and the value of A_p will be set to the same values as those used in Fig. 7(a) in the manuscript. Here, we will only study the off-resonant PDC process, as on-resonant pulsed PDC is a well-studied problem, and also, it is the off-resonant PDC process that leads to the generation of the light-matter entangled state. The pump slowly varying envelope is chosen Gaussian, and it is defined as $\mathcal{E}(t) = e^{-\frac{(t-t_0)^2}{2\tau_p^2}}$. τ_p is the length of the pulse. The full width at half maximum (FWHM) of the pulse bandwidth is

$$\Delta\omega_{\text{FWHM}} = \frac{2.355}{\tau_p}.$$

For the case shown in Fig. 7(a), the pump frequency ω_p is detuned by 30Ω from the resonance condition $\omega_p = \omega_s + \omega_i$, i.e., $\Delta_1 = 30\Omega$. The length of the pulse is $\tau_p = \frac{2.545}{\Omega}$ in Fig. 7(a), the spectral width of the pulse is $\Delta\omega_{\text{FWHM}} = 0.93\Omega$, such that even half of the spectral bandwidth, $\Delta\omega_{\text{FWHM}}/2$, remains much smaller than the detuning Δ_1. This means that the entire spectral components of the pulse lie far away from the energy-conserving condition. Consequently, none of the frequency components of the pump pulse can efficiently satisfy energy conservation for the PDC process, and the down-conversion interaction remains strongly off-resonant throughout the pulse duration. For the current case, if we pumped the nonlinear cavity, we get the output state of the form shown in the Fig S4: The photonic states $|\phi_n\rangle$

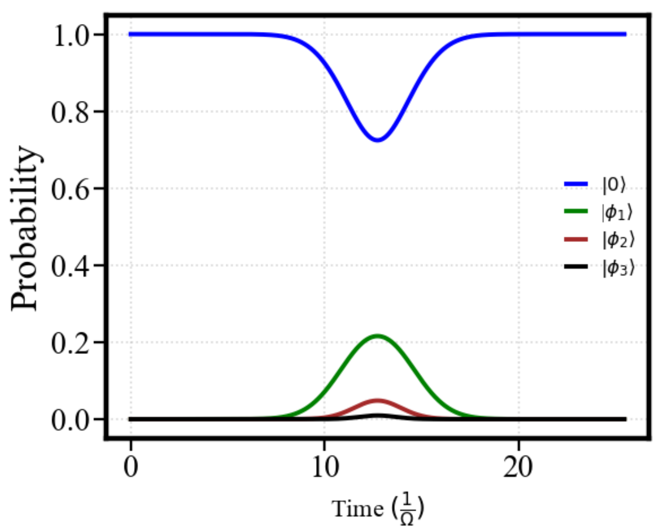

Figure S4: Temporal evolution of photonic states $|\phi_n\rangle$ under off-resonant pulsed PDC process.

exhibit transient behavior; they are populated only during the temporal window in which the pump pulse interacts with the nonlinear medium. Since the PDC process is far off-resonant, these states do not accumulate population permanently. As the pump amplitude decays to zero, the excitation amplitudes of these photonic states also vanish, leaving no residual population. Next, we will derive the mathematical expression for the probability amplitude of the state $|\phi_1\rangle$ and show the expression matches the behaviour shown in Fig S4. The probability amplitude for the generation of the state $|\phi_1\rangle$ is calculated using the perturbative approach by keeping only the first-order term because the probabilities of higher-order excitation processes are vanishingly small and can therefore be neglected. We again consider the nonlinear interaction Hamiltonian $\hat{H}_{NL}(t)$ introduced in the manuscript and also above. We assume the system starts in the multimode vacuum $|0,0,0,0\rangle = |0\rangle$ and work in the *low-gain* (first-order) regime, so only the pair-creation terms contribute.

a. First-order state. The first-order Dyson expansion gives $\left|\psi^{(1)}(t)\right\rangle = |0\rangle - \frac{i}{\hbar}\int_{-\infty}^{t} \mathrm{d}t'\, \hat{H}_{\text{NL}}(t')\, |0\rangle$. Since the annihilation terms in the Hamiltonian $\hat{H}_{NL}(t)$ annihilate the vacuum, only the creation terms survive, yielding the single-pair amplitudes

$$c_1(t) \equiv \langle 1,0,0,1|\psi^{(1)}(t)\rangle \approx -iA_p \int_{-\infty}^{t} \mathrm{d}t'\, E_0(t')\, e^{-i\Delta_1 t'}\,, \tag{S65}$$

$$c_2(t) \equiv \langle 0,1,1,0|\psi^{(1)}(\tau)\rangle \approx -iA_p \int_{-\infty}^{t} \mathrm{d}t'\, E_0(t')\, e^{-i\Delta_1 t'}\,. \tag{S66}$$

It is convenient to define the common pump integral $\mathcal{I}(t) \equiv \int_{-\infty}^{t} \mathrm{d}\tau'\, E_0(t')\, e^{-i\Delta_1 t'}$. Such that $c_1(t) = c_2(t) = -iA_p\mathcal{I}(t)$

b. Projection onto the $|\phi_1\rangle$ state. The state $|\phi_1\rangle$ has the form:

$$|\phi_1\rangle \;\equiv\; \frac{1}{\sqrt{2}}\Big(\,|1,0,0,1\rangle + |0,1,1,0\rangle\,\Big). \tag{S67}$$

Its overlap with $\big|\psi^{(1)}(t)\big\rangle$ is

$$\langle\phi_1|\psi^{(1)}(t)\rangle = \frac{1}{\sqrt{2}}\big(c_1(t) + c_2(t)\big) = -i\,\mathcal{I}(t)\,\sqrt{2}A_p. \tag{S68}$$

Therefore, the probability to be in $|\phi_1\rangle$ at time t is $P_{\phi_1}(t) \;\propto\; 2\big|A_p|^2\,\big|\mathcal{I}(t)\big|^2$. The smooth, non-oscillatory behavior of the curve without the characteristic oscillations of period $\frac{1}{\Delta_1}$ arises from the presence of the pump integral $\mathcal{I}(t)$. In a given time interval, the probability of exciting the $|\phi_1\rangle$ state is proportional to $|\mathcal{I}(t)|^2 = \mathcal{I}(t)\mathcal{I}^*(t) = \int_{-\infty}^{t}\mathrm{d}t' \int_{-\infty}^{t}\mathrm{d}t''\, E_0(t')E_0(t'')\, e^{-i\Delta_1(t'-t'')}$. This double integral contributes significantly only when $t' \approx t''$; for $t' \neq t''$, the rapidly oscillating phase factor causes destructive interference, canceling out the contributions. As a result, the fast oscillations are effectively averaged out, leading to a smooth, slowly varying probability that follows the envelope of the pump pulse.

S8. EXPERIMENTAL CAVITY-QED PARAMETERS

In Table S1, we summarize experimentally reported cavity-QED parameters from representative state-of-the-art optical cavity-QED experiments. The experimentally reported parameters (g, κ, γ) are identified with $(\Omega, \gamma_i/2, \Gamma_e/2)$ in our notation. Here, $\Omega \equiv g$ denotes the atom–field coupling strength, κ is the half-linewidth (field decay rate) of the cavity mode, whereas $\gamma_{i,s}$ denotes the corresponding full cavity linewidth (photon-number decay rate). Likewise, γ is the atomic polarization (dipole) decay rate, whereas Γ_e is the atomic spontaneous-emission (population) decay rate. The idler-mode decay rate γ_i is used since the idler cavity modes are directly coupled to the atomic transitions. The selected works span a variety of optical cavity-QED platforms, including neutral atoms and trapped ions, and provide benchmarks for currently achievable atom–cavity coupling strengths and decay rates.

Table S1: Comparison of experimentally reported cavity-QED parameters with the notation used in this work. Here, $g \equiv \Omega$, $2\kappa \equiv \gamma_i$, and $2\gamma \equiv \Gamma_e$.

Reference	$\frac{g}{2\pi}$ (MHz)	$\frac{\kappa}{2\pi}$ (MHz)	$\frac{\gamma}{2\pi}$ (MHz)	$\frac{2\kappa}{g}$ ($\equiv \frac{\gamma_i}{\Omega}$)	$\frac{2\gamma}{g}$ ($\equiv \frac{\Gamma_e}{\Omega}$)
Wang *et al.* (2025) [S3]	2.62	1.1	2.6	0.84	1.98
Grinkemeyer *et al.* (2025) [S4]	100	32.5	3	0.65	0.06
Liu *et al.* (2023) [S5]	3.2	1.0	2.6	0.62	1.62
Thomas *et al.* (2022) [S6]	5.4	2.7	3.0	1.0	1.12
Deist *et al.* (2022) [S7]	2.7	0.53	3.0	0.39	2.22
Specht *et al.* (2011) [S8]	5.0	2.5	3.0	1.0	1.2
Maunz *et al.* (2004) [S9]	16.0	1.4	3.0	0.175	0.375
Kimble *et al.* (1999) [S10]	32.0	4.0	2.6	0.25	0.16
Kimble *et al.* (1998) [S11]	120.0	40.0	2.6	0.67	0.043

[S1] E. Brion, L. H. Pedersen, and K. Mølmer, Adiabatic elimination in a lambda system, Journal of Physics A: Mathematical and Theoretical **40**, 1033–1043 (2007).

[S2] D. A. Steck, *Rubidium 87 D Line Data (revision 1.6)*, Los Alamos National Laboratory, Theoretical Division (T-8), Los Alamos, NM (2003), revision 1.6 (14 October 2003). Available at `https://steck.us/alkalidata/rubidium87numbers.1.6.pdf`.

[S3] Z. Wang, S. Guan, G. Teng, P. Yang, P. Zhang, G. Li, and T. Zhang, A cavity qed system with defect-free single-atom array strongly coupled to an optical cavity, Quantum Frontiers **4**, 10 (2025).

[S4] B. Grinkemeyer, E. Guardado-Sanchez, I. Dimitrova, D. Shchepanovich, G. E. Mandopoulou, J. Borregaard, V. Vuletić, and M. D. Lukin, Error-detected quantum operations with neutral atoms mediated by an optical cavity, Science **387**, 1301 (2025), https://www.science.org/doi/pdf/10.1126/science.adr7075.

[S5] Y. Liu, Z. Wang, P. Yang, Q. Wang, Q. Fan, S. Guan, G. Li, P. Zhang, and T. Zhang, Realization of strong coupling between deterministic single-atom arrays and a high-finesse miniature optical cavity, Phys. Rev. Lett. **130**, 173601 (2023).

[S6] P. Thomas, L. Ruscio, O. Morin, and G. Rempe, Efficient generation of entangled multiphoton graph states from a single atom, Nature **608**, 677 (2022).

[S7] E. Deist, Y.-H. Lu, J. Ho, M. K. Pasha, J. Zeiher, Z. Yan, and D. M. Stamper-Kurn, Mid-circuit cavity measurement in a neutral atom array, Phys. Rev. Lett. **129**, 203602 (2022).

[S8] H. P. Specht, C. Nölleke, A. Reiserer, M. Uphoff, E. Figueroa, S. Ritter, and G. Rempe, A single-atom quantum memory, Nature **473**, 190 (2011).

[S9] P. Maunz, T. Puppe, I. Schuster, N. Syassen, P. W. H. Pinkse, and G. Rempe, Cavity cooling of a single atom, Nature **428**, 50 (2004).

[S10] J. Ye, D. W. Vernooy, and H. J. Kimble, Trapping of single atoms in cavity qed, Phys. Rev. Lett. **83**, 4987 (1999).

[S11] C. J. Hood, M. S. Chapman, T. W. Lynn, and H. J. Kimble, Real-time cavity qed with single atoms, Phys. Rev. Lett. **80**, 4157 (1998).